Theor Appl Climatol (2009) 97:29–40
DOI 10.1007/s00704-008-0071-z

SPECIAL ISSUE

A review of interdecadal changes in the nonlinearity of the El Niño-Southern Oscillation

Soon-Il An

Received: 21 March 2008 / Accepted: 2 October 2008 / Published online: 29 October 2008

Abstract Many features of the El Niño-Southern Oscillation (ENSO) display significant interdecadal changes. These include general characteristics such as amplitude, period, and developing features, and also nonlinearities, especially the El Niño-La Niña asymmetry. A review of previous studies on the interdecadal changes in the ENSO nonlinearities is provided. In particular, the methods for measuring ENSO nonlinearities, their possible driving mechanisms, and their interdecadal changes are discussed. Two methods for measuring ENSO nonlinearities are introduced; the maximum potential intensity, which refers to the upper and lower bounds of the cold tongue temperature, and the skewness, which represents the asymmetry of a probability density function. For example, positive skewness (a strong El Niño vs. a weak La Niña) of the tropical Pacific sea surface temperature (SST) anomalies is dominant over the eastern tropical Pacific, with an increase seen during recent decades (e.g., 1980–2000). This positive skewness can be understood as a result of several nonlinear processes. These include the warming effect on both El Niño and La Niña by nonlinear dynamic heating (NDH), which intensifies El Niño and suppresses La Niña; the asymmetric negative feedback due to tropical oceanic instability waves, which has a relatively stronger influence on the La Niña event; the nonlinear physics of the ocean mixed layer; the Madden-Julian-Oscillation/Westerly-Wind-Burst and ENSO interaction; the biological-physical feedback process; and the nonlinear responses of the tropical atmospheric convection to El Niño and La Niña conditions. The skewness of the tropical eastern Pacific SST anomalies and the intensities of the above-mentioned mechanisms have both experienced clear decadal changes in a dynamically associated manner. In particular, there is a dynamic linkage between the decadal changes in the El Niño-La Niña asymmetry and those in NDH. This linkage is based on the recent decadal changes in mean climate states, which provided a favorable condition for thermocline feedback rather than for zonal advection feedback, and thus promoted the eastward propagation of the ENSO-related atmospheric and oceanic fields. The eastward propagating ENSO mode easily produces a positive NDH, resulting in asymmetric ENSO events in which El Niño conditions are stronger than La Niña conditions.

S.-I. An (✉)
Department of Atmospheric Sciences, Yonsei University,
Seoul 120-749, Korea
e-mail: sian@yonsei.ac.kr

1 Introduction

The El Niño-Southern Oscillation (ENSO) is known as the most prominent interannual variability in the global climate system, and it has global climatic, ecological, and social impacts (Cane 1983; Philander 1983; Rasmusson and Wallace 1983). A strong atmosphere–ocean coupling involving a dominant trade wind in the equatorial tropical Pacific, the zonal thermal contrast between the warm pool in the tropical western Pacific and the cold tongue in the tropical eastern Pacific, and a shallow thermocline in the eastern Pacific, all contribute to a coupled instability that evokes ENSO. A great deal of progress has been made in understanding and predicting ENSO (Cane and Zebiak 1985; Cane et al. 1986; Zebiak and Cane 1987; Schopf and Suarez 1988; Battisti and Hirst 1989; Philander 1990; Jin and Neelin 1993; Neelin et al. 1994, 1998). In particular, linear theories have provided an understanding of the mechanisms that lead the oscillatory nature of ENSO and its periodicity of about 3–6 years. A small perturbation in the

tropical climate system can easily grow and develop into either El Niño or La Niña, through the so-called 'Bjerknes feedback' (Bjerknes 1966). The transition between an El Niño event and a La Niña event occurs through a delayed negative feedback of ocean dynamic adjustment (Cane and Zebiak 1985; Wyrtki 1985; Cane et al. 1986; Zebiak and Cane 1987; Schopf and Suarez 1988; Battisti and Hirst 1989; Philander 1990; Jin and Neelin 1993; Neelin et al. 1994, 1998; Jin 1996, 1997; An and Kang 2000; An and Jin 2001). An example of this phase reversal is when the equatorial upper-ocean heat content slowly drains out (builds up) during a warm (cold) ENSO phase, as a result of the dynamic mass exchange between the equatorial belt and the off-equatorial regions (Jin 1996, 1997).

Delayed negative feedback currently provides the best representation for the basic mechanism of ENSO-like oscillation. In prototype linear models, such as the delayed oscillator model (Suarez and Schopf 1988; Schopf and Suarez 1988; Battisti and Hirst 1989) or the recharge oscillator model (Jin 1996, 1997; Jin and An 1999), ENSO is portrayed as having a regular and periodic oscillatory mode over various parameter ranges. However, observed ENSOs are irregular and quasi-periodic, with an amplitude locked to the annual cycle. These observed characteristics of ENSO may be attributed to either nonlinear dynamics (Jin et al. 1994; Tziperman et al. 1994) or to stochastic forcing (Chang et al. 1994; Penland and Sardeshmukh 1995; Thompson and Battisti 2000). The El Niño-La Niña asymmetry and its interdecadal change are not well understood, despite the significance of this nonlinear process in influencing ENSO statistics.

Wu and Hsieh (2003) objectively identified the El Niño-La Niña asymmetry by using nonlinear canonical correlation analysis. An (2004) computed the leading eigenmode of the El Niño-La Niña asymmetry using monthly-mean global sea surface temperature (SST) data spanning from 1864 to the present. Both studies verified that the ENSO asymmetry underwent significant interdecadal changes. Interestingly, the interdecadal changes in the ENSO nonlinearity during the recent half century mirrored the changes in the characteristics of ENSO such as its intensity, period, predictability, propagating feature, and onset (e.g., Wang 1995; Kirtman and Schopf 1998; An and Wang 2000; Ye and Hsieh 2006). This implies a dynamic linkage between these changes. One possible dynamic linkage for interdecadal changes is proposed by Timmermann et al. (2003). They asserted that nonlinearities in the tropical Pacific heat budget could lead to a bursting behavior in the decadal occurrences of strong El Niño events, called 'El Niño bursting'. Alternatively, changes in ENSO nonlinearity could be related to changes in the background climate state (An and Jin 2004). Both the lower-order (linear) statistics of ENSO and its higher-order (nonlinear) statistics, such as 'skewness', can be modified by changes in the background climate state. Nonlinear mechanisms in the tropical coupled ocean-atmospheric system, and their effects on the El Niño-La Niña asymmetry and its interdecadal changes, may explain why strong El Niño events, such as the 1982/1983 and 1997/1998 episodes, occurred frequently and with great intensity during recent decades but were rare during earlier decades.

This paper is a review of the interdecadal changes in ENSO nonlinearity. In Sect. 2, measurements of the nonlinearity of ENSO are introduced. Section 3 presents the nonlinear dynamic processes that lead to the warm/cold asymmetry of ENSO. Section 4 investigates the causes of the interdecadal changes in ENSO nonlinearity. A summary and discussion are given in Sect. 5.

2 Measuring the nonlinearity of ENSO

During El Niño events, warm SST anomalies over the cold tongue region (the tropical eastern Pacific) frequently reached above 5°C compared to normal years, while cold SST anomalies during the subsequent La Niña events had relatively smaller amplitudes. This warm/cold asymmetry in an ENSO cycle provides an ideal example of the nonlinearity in ENSO. Some qualitative and quantitative measures of the nonlinearity of ENSO are discussed in this section.

2.1 Maximum Potential Intensity (MPI)

The maximum potential intensity (MPI) of the ENSO refers to an upper and lower bound of the cold tongue temperature (Jin et al. 2003). For example, the warm pool temperature (tropical western Pacific SST) is the highest SST on the global ocean, and is bounded by the radiative-convective equilibrium temperature (Waliser and Graham 1993) of about 30°C. Theoretically, the cold tongue temperature cannot go beyond the warm pool temperature; thus, the warm pool temperature is the upper bound of the cold tongue temperature and is the MPI for El Niño events. Similarly, the lower bound of the cold tongue temperature, the MPI for La Niña events, is about 20°C, corresponding to a complete surface outcropping of the thermocline. Thus, the cold tongue SST may vary between 20 and 30°C. Obviously, this range will vary with climate changes.

The El Niño (La Niña) refers to abnormal warming (cooling) over the 'cold tongue' region. Here, 'abnormal' does not mean a slightly perturbed state from normal, but instead indicates a distinctive change from the normal climate state, such as when the cold tongue temperature increases up to the warm pool temperature, i.e., the MPI of El Niño. As shown in Fig. 1, the cold tongue temperature

during a strong El Niño almost reaches the climatologic warm pool temperature. One of the best examples of this was the 1997/98 El Niño, which was the strongest El Niño event ever instrumentally observed (McPhaden 1999). During the winter of 1997–98, the warm pool expanded so far to the east that the climatologic cold tongue vanished and its temperature reached more than 28°C. In addition, the climatological tilt of the thermocline was reversed, and the equatorial undercurrent was significantly disrupted (see Fig. 2 of An and Jin 2004). Thus, the normal climate states of the ocean and atmosphere completely collapsed during the mature phase of this 1997/98 El Niño event. This cannot be explained by a linear mechanism.

2.2 Statistical measure (skewness)

Skewness is a statistical measure of the ENSO nonlinearity (Burgers and Stephenson 1999), and represents the asymmetry of a probability density function (Fig. 2), which is zero for a normal distribution (White 1980). The moment coefficient of skewness is defined as the normalized third statistical moment

$$skewness = \frac{m_3}{(m_2)^{3/2}} \tag{1}$$

where m_k is the *kth* moment

$$m_k = \sum_{i=1}^{N} \frac{(x_i - \overline{X})^k}{N}$$

and where x_i is the *ith* observation, $\overline{X}$ is the mean, and N is the number of observations.

The skewness of various ENSO indices are summarized in Table 1. The SST data spanning from 1950 to 2003 are obtained from the NCEP (National Center for Environmental Prediction) reconstructed monthly-mean SST data (Reynolds and Smith 1994). The data are constructed by applying the optimal reanalysis method, using marine-surface observations and satellite AVHRR data. The anomalies are calculated by removing the climatological mean. The skewness of the Niño-3 index (the SST anomaly averaged over 5°N-5°S and 90–150°W) is positive, indicating that the warm SST anomaly in the equatorial eastern Pacific is stronger than the cold SST anomaly. Likewise, El Niño is stronger than La Niña. A negative skewness is recorded for the Niño-4 index (5°N–5°S, 150°W–160°E), where the SST anomaly is usually opposite to that in the eastern Pacific. The table also shows a strong decadal change in the skewness, which will be discussed later.

Figure 3 shows the skewness of SST anomalies over the tropical Pacific Ocean. There is a strong positive skewness over the central to eastern Pacific and a weak negative skewness over the subtropical western Pacific. A similar skewness pattern was also found in a long-term simulation of the coupled general circulation model. The skewness distribution appears to be directly related to the ENSO pattern during the mature phase, implying that the amplitude of the warm SST anomaly is larger than that of the cold SST anomaly.

3 Possible causes of El Niño-La Niña asymmetry

Having introduced the nonlinearity of ENSO in the previous section, this section will examine possible causes of the El Niño-La Niña asymmetry, in particular why El Niño events are frequently larger than La Niña events.

3.1 Nonlinear dynamic heating (NDH)

An analysis of the heat budget of the ocean surface layer is used to investigate the El Niño-La Niña asymmetry. The temperature tendencies in the ocean surface layer can be calculated with the following equation:

$$\frac{\partial T'}{\partial t} = -\begin{pmatrix} u'\partial x\overline{T} + v'\partial y\overline{T} + w'\partial z\overline{T} \\ +\overline{u}\partial xT' + \overline{v}\partial yT' + \overline{w}\partial zT' \end{pmatrix} - (u'\partial xT' + v'\partial yT' + w'\partial zT') + R' \tag{2}$$

where T, u, v, and w are SST, zonal, meridional, and vertical velocities, respectively. The overbar and prime denote the

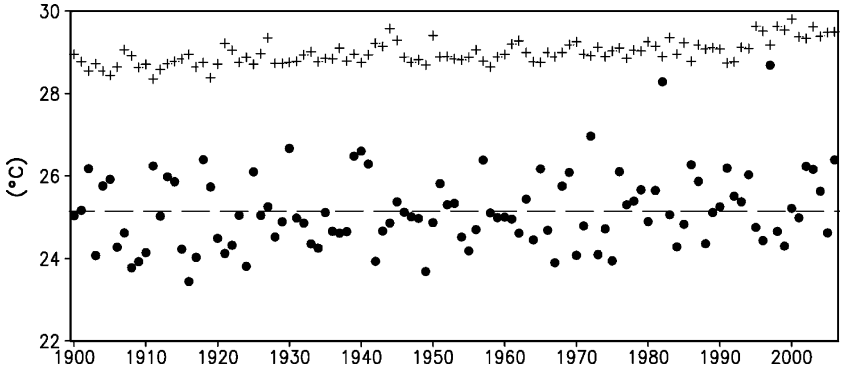

Fig. 1 Time series of winter mean (Dec–Feb) SST in the warm pool (*cross*; averaged over the area 5°N–5°S, 130–160°E) and in the cold tongue (*closed dot*; averaged over the area 5°N–5°S, 120–90°W)

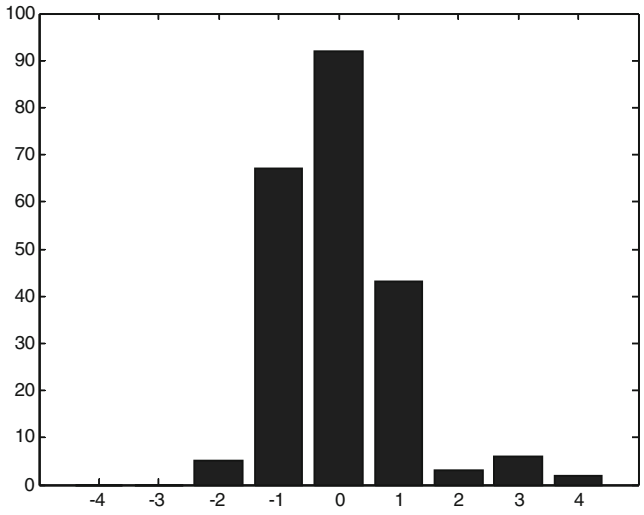

Fig. 2 Histogram of the Niño-3 index for 1950–2003

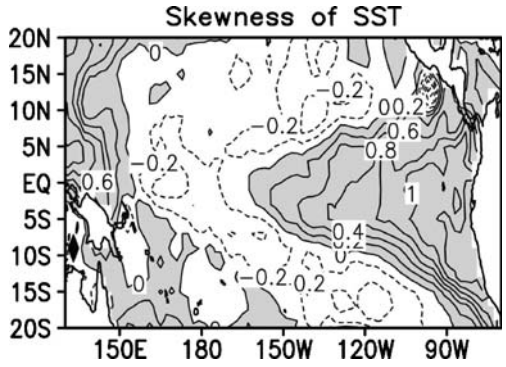

Fig. 3 Skewness distribution of SST anomalies for 1950–2003. Positive values are *shaded*

climatologic mean and anomalies, respectively. The surface heat flux and the sub-grid scale contributions (e.g., small oceanic diffusion, or the heat flux due to a tropical instability wave) are attributed to the residual term *R*. The terms within the first parentheses represent the linear dynamic thermal advections, and the terms within the second parentheses represent the nonlinear dynamic thermal advections (or the nonlinear dynamic heating, NDH).

An and Jin (2004) performed a theoretical analysis using the low-order ENSO model, in which the nonlinear effects were represented by the zonal and vertical dynamic thermal advection terms in the SST equation. The low-order nonlinear ENSO model produced the warm/cold asymmetric ENSO, and also produced decadal occurrences of strong El Niño (warm) events, the so-called 'bursting behavior' (Timmermann et al. 2003) across a broad model parameter range. In particular, the strong warm events (El Niño bursting) are accompanied by a strong warming tendency due to NDH, ultimately generating the El Niño-La Niña asymmetry.

To evaluate the role of NDH, we performed the heat budget analysis in the uppermost 50-m layer of the tropical eastern Pacific using SODA ocean assimilation data (Carton et al. 2000) (similar results are also found in An and Jin (2004), who used the NCEP ocean assimilation data). SODA data consist of monthly-mean ocean temperature, horizontal current, salinity, wind stress, and sea-level pressure, with a horizontal resolution of 1.5×1° and a vertical resolution of 10 m in the upper 100 m of depth. The heat budget was calculated for either a fixed mixed-layer depth of 50 m, or for a varying mixed-layer depth as shown in Wang and McPhaden (2000). Both results are similar to each other, indicating that the budget analysis is quite robust.

Table 1 Skewness of ENSO indices for various decadal periods

	Pre 1980s (1950–70)	Post 1980s (1980–99)	1950–2003
Niño-3	0.17	0.99	0.64
Niño-3.4	0.10	0.35	0.21
Niño-4	−0.24	−0.63	−0.18

Figure 4 shows the SST anomalies (upper panels) and the heating rate due to NDH (lower panels) for the 1997/98 El Niño (July 1997–May 1998), and for the subsequent 1998/99 La Niña (July 1998–May 1999). NDH contributed to a positive warming of about 2°C/month over the central/eastern equatorial Pacific during both El Niño and La Niña, so it served to amplify the El Niño events but to weaken the La Niña events. The warming tendency due to NDH during other strong El Niño events (for example, during 1972–73 and 1982–83) and the subsequent La Niña events were also observed (Fig. 5). Furthermore, by analyzing the atmosphere–ocean coupled model outputs, An et al. (2005) showed using coupled general circulation (GCM) models that positively skewed ENSO were commonly accompanied by a warming tendency due to NDH.

Figure 5 shows the time evolution of the SST tendencies due to NDH, together with the SST anomalies. These data are averaged over the region of 150–90°W and 1°N-1°S, and span from 1950–2001. In this calculation, two ocean assimilation data sets are used (SODA and NCEP). To remove the shorter time-scale fluctuations, a 3-month running average is applied. As seen in the figure, the SST tendency due to NDH is positive throughout the whole data period. Peaks are recorded during the strong El Niño episodes of 1982/83 and 1997/98, lagging a few months behind the peak SST anomalies. The amplitudes of these strong ENSO events are strongly skewed toward the warm event. On the contrary, during the modest and weak ENSO events, such as during 1986/87, NDH is negligible (Jin et al. 2003; An and Jin 2004). Both the observations and the coupled GCM show a significant positive correlation between the NDH and the amplitude of the ENSO (An et al. 2005a). An and Jin (2004) mentioned that the most

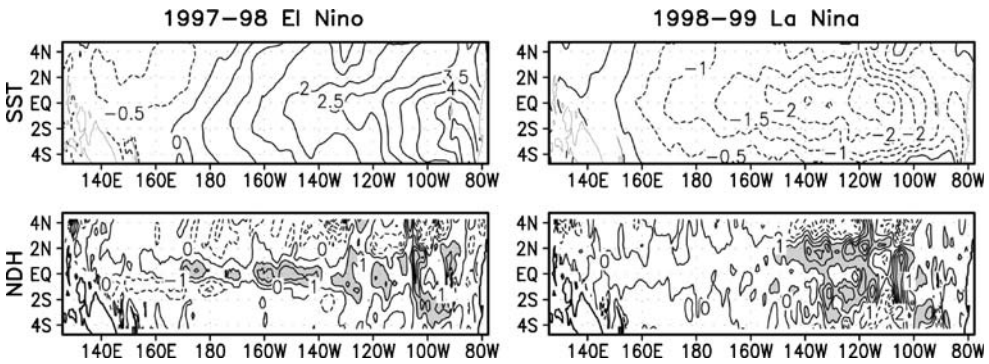

Fig. 4 SST anomaly (°C) and rate of change in SST (°C/month) due to the nonlinear dynamical heating during the 1997/98 El Niño (*left panel*) and the 1998/99 La Niña (*right panel*). Greater than 1 (°C/month) of NDH are *shaded*

significant contribution to NDH is from the vertical advective heating, with a secondary contribution from the zonal advective heating. In the coupled GCM, the larger warming El Niño events are also accompanied by the larger NDH (An et al. 2005a).

3.2 Tropical instability waves

Tropical instability waves (TIWs) are unique features observed in the tropical Pacific and Atlantic Oceans. They have periods of 20–40 days, and their length is on the order of 1,000 km (Legeckis 1977; Weisberg and Weingartner 1988). TIWs arise from either barotropic instability (Qiao and Weisberg 1998) or baroclinic instability (Hansen and Paul 1984; Wilson and Leetmaa 1988) in the mean climate states; thus, the variability and structure of TIWs are closely related to the position and strength of equatorial cold tongues and zonal currents. For example, the warming effect, in particular the meridional eddy heat flux induced by TIWs (Swenson and Hansen 1999), becomes strongest during the coolest cold-tongue season (August to January). TIWs significantly contribute to the observed interannual variability; thus, it can be inferred that the ENSO could be modified by TIWs (Jochum and Murtugudde 2004).

During La Niña, an increased meridional SST gradient and an intensified current near the eastern equatorial Pacific accompany a strong variability of TIWs (Yu and Liu 2003). By mixing warm off-equatorial water (eastern-north Pacific warm pool) with cold equatorial water (equatorial eastern Pacific cold tongue), active TIWs prevent the equatorial cold-tongue from cooling further. On the contrary, TIW activity is suppressed during El Niño, due to the reduced meridional temperature gradient (Philander 1990; Vialard et al. 2001). This results in less modification of the cold-tongue temperature by TIWs. On the whole, the TIW reduces the cold-tongue intensity. However, its effect is relatively stronger during La Niña than during El Niño.

The volume-averaged zonal, meridional, and vertical thermal advections over the Niño-3 region (5°S–5°N, 150–90°W), and in the upper 50 m depth of the ocean surface, were computed. An (2008) obtained a similar result by computing the heat budget over the Niño-3.4 region (5°S–5°N, 120–170°W). The vertical velocity has been calculated based on the continuity equation; thus, thermal advections could be replaced by heat flux convergence. The dynamic heat flux convergence (HFC) due to TIWs was calculated by the following formula:

$$HFC = \int_{x=150^\circ W}^{90^\circ W}\int_{y=5^\circ S}^{5^\circ N}\int_{z=50}^{0} -\left(\frac{\partial(u'T')}{\partial x}+\frac{\partial(v'T')}{\partial y}+\frac{\partial(w'T')}{\partial z}\right) dxdydz \Big/ \iiint dxdydz \quad (3)$$

The time series of the HFC anomaly is shown together with the time series of the Niño-3 index in Fig. 6, after the seasonal cycle of the HFC (which modifies the seasonal SST budget) has been removed. A positive HFC indicates

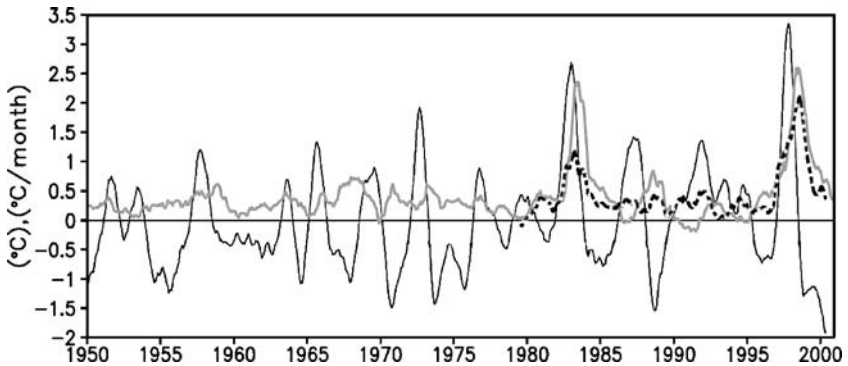

Fig. 5 Time series of SST tendencies (°C/month) due to the nonlinear dynamical heating averaged over 5°N-5°S, 150–90°W obtained from the NCEP ocean assimilation data (*dashed line*) and SODA ocean assimilation data (*light solid line*). The *solid line* indicates the SST anomaly (°C) averaged over the same region

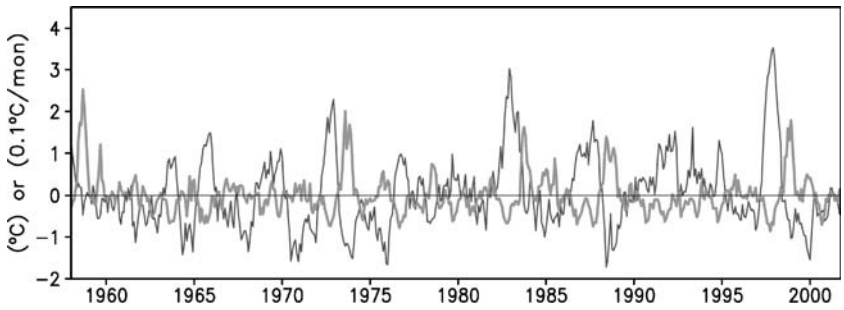

Fig. 6 Time series of Niño-3 index (*solid line*) and three-dimensional heat flux convergence due to TIW over the Niño-3 region (*dash-dotted line*)

warming in the Niño-3 region, and vice versa. The general range of the HFC is between −0.1 and 0.2°C/month, and the warming tendency is twice the cooling tendency. There is a clear out-of-phase relationship between Niño-3 and the HFC, since the heat flux due to TIW usually reduces the amplitude of Niño-3. This results in a negative feedback on ENSO. It should be noted that the cooling tendency during El Niño is weaker than the warming tendency during La Niña, even though the corresponding Niño-3 amplitude for El Niño is larger than that for La Niña. This implies that the warming tendency by HFC associated with decreasing SSTs during La Niña is greater than the cooling tendency by HFC associated with increasing SSTs during El Niño. As an example, when the Niño-3 SST anomaly increased by 1°, the SST tendency induced by HFC due to TIW became −0.086°C/month. Conversely, when the Niño-3 SSTA decreased by 1°, the SST tendency due to TIW became 0.128°C/month. Obviously, the skewness (in which El Niño is stronger than La Niña) is in part attributable to the asymmetric development of TIW with respect to changes in the cold tongue temperature. The positive SST tendency induced by HFC due to TIW effectively hinders the development of La Niña, while the negative SST tendency is less effective in blocking the development of El Niño. Consequently, the amplitude of El Niño can be larger than that of La Niña.

3.3 Other nonlinear processes

The mixed-layer formation is a highly nonlinear process. In the upper ocean, vertical mixing is constrained by the stratification of the vertical mean temperature profile (Galanti et al. 2002). The stably stratified vertical temperature distribution (the strong vertical temperature/density gradient), which is pronounced especially during La Niña, obstructs the vertical mixing. Conversely, during El Niño, the deepening of the thermocline leads to a low vertical temperature gradient, which may allow active vertical mixing. Thus, the vertical mixing that plays an important role in a mixed layer formation depends on the background climate condition, and it in turn modifies the background climate state. The actual role of a mixed layer in modifying the ENSO nonlinearity needs to be explored in the future.

Kessler and Kleeman (2000) suggested that the intraseasonal oscillation in the tropics could interact constructively with the ENSO cycle through nonlinear rectification, and that rectified SST anomalies cause a stronger El Niño. Furthermore, Eisenman et al. (2005) mentioned that the SST associated with ENSO modulates the westerly-wind-burst (WWB) in a nonlinear way, after which ENSO responds linearly to the modulated events. This multiplicative stochastic forcing can modify the shape of the probability density function of ENSO, as in Fig. 2. The relationship between this multiplicative stochastic process and the El Niño-La Niño asymmetry, and its quantitative role in generating the asymmetric ENSO, need to be explored in the future.

Timmermann and Jin (2002b) asserted that the biological-physical feedback in the eastern equatorial Pacific causes ENSO asymmetry. The phytoplankton blooms in the eastern equatorial Pacific that absorb a lot of solar energy tend to occur during La Niña conditions, because of intensified oceanic upwelling. El Niño conditions are characterized by low chlorophyll concentrations due to suppressed oceanic upwelling. This feedback in the eastern equatorial Pacific plays a role in damping La Niña events, but has less of an effect on modifying El Niño events, leading to the El Niño-La Niña asymmetry.

Kang and Kug (2002) demonstrated that the relatively weak SST anomaly during La Niña compared to that during El Niño is attributable to the nonlinear response of zonal wind stress anomalies to both events; that is, the weak La Niña SST anomalies promote wind-stress anomalies westward by about 10–15 longitudinal degrees, compared with El Niño. This results in a weaker La Niña event; the zonal location of the wind stress anomalies influences the amplitude of ENSO event by modifying the ocean adjustment timescale (e.g., An and Wang 2000). Similarly, Hoerling et al. (1997) mentioned nonlinear features in the thermodynamic control of deep convection, in which the tropical rainfall anomalies associated with El Niño and La Niña are located east of the dateline during warm events, but west of the dateline during cold events.

Conversely, Schopf and Burgman (2006) evoked a cautionary note on the use of time mean statistics in the attempt to understand relationships between the mean SST and ENSO, since the larger ENSO cycles lead to statistics that show a flatter looking time mean thermocline purely by kinematic effects. In other words, a change in the statistics of the long-term mean temperature may be seen even with an absence of diabatic effects. Thus, there is a kinematic effect due to oscillating a nonlinear ocean temperature profile with finite-amplitude excursions. This possibly causes the Eulerian time mean temperature to rise (fall) in cases where the curvature of the temperature is positive (negative) as the amplitude of the oscillations increases (Schopf and Burgman 2006).

4 Interdecadal changes in the ENSO nonlinearity

4.1 Interdecadal changes in El Niño-La Niña asymmetry

In order to explore the long-term changes of the ENSO nonlinearity, the 21-year moving-window skewness of the Niño-3 index is calculated using the Extended Reconstruction SST version 2 (Smith and Reynolds 2004). As seen in Fig. 7, the skewness of ENSO underwent interdecadal variations. Positive skewness appears during the 1930s, in the years 1960–1975 (weak), and in the years 1975–2000 (strong). The negative skewness occurs during 1905–1930 and during 1940–1955. In particular, the positive skewness dominates during the recent decades, as strong El Niño events have occurred frequently during this time. Note that the ENSO events during the positive skewness decades are more predictable than they are during the negative skewness decades (1865–1875 and 1916–1975) (An 2004).

An (2004) identified the dominant pattern of the long-term changes of the El Niño-La Niña asymmetry by applying a principal component analysis (PCA) to the 21-year moving-window skewness of the tropical Pacific SST. The first PCA mode (see Fig. 1 of An (2004)) is characterized by a tongue-shaped pattern centered at the equatorial eastern Pacific and by small negatives in the equatorial central and northwestern Pacific. These represent the asymmetry between El Niño (warm event) and La Niña (cold event). The corresponding principal component (PC) time series is very similar to the 21-year moving-window skewness of the Niño-3 index shown in Fig. 7.

4.2 Zonal propagation of ENSO and El Niño-La Niña asymmetry

In the previous section, it was mentioned that NDH could lead to the El Niño-La Niña asymmetry. According to An and Jin (2004), the amplitude of NDH is related to the propagation characteristics of ENSO, such that the eastward propagating ENSO tends to produce large NDH, while the westward propagating ENSO barely produces NDH. This is because the eastward-propagating ENSO provides a favorable phase relationship between temperature and current, resulting in the strong NDH warming. Thus, any changes in the zonal propagating features of ENSO, by modifying NDH, can influence the El Niño-La Niña asymmetry. As observed, the eastward propagating tendency appearing in the equatorial SST anomaly has been dominant since the late 1970s, which coincides with strong El Niño-La Niña asymmetry. Conversely, the decadal periods 1930–1950s and 1950s–1970s, when the westward propagating tendency of ENSO was dominant, are marked by weak or negative skewness (Table 2, or Fig. 2 of An (2004)). Thus, the ENSO events that occurred during the decades with positive skewness of the Niño-3 index tend to propagate eastward.

4.3 Unification of mechanisms on the decadal change in ENSO characteristics

An and Wang (2000) have studied the decadal changes in ENSO by examining long-term observations as well as ocean assimilation data. As summarized in Table 2, they found that the ENSO period increased from 3–4 years (high frequency) during 1962–1975, to 4–6 years (low frequency) during 1980–1999. This latter time period was accompanied by a significant change in the structure of the coupled ENSO mode, such as the eastward shift of the westerly anomalies, the meridional expansion of the anomalous surface wind pattern, and the weaker intensity of the easterly anomalies in the eastern Pacific. In addition, the aforementioned interdecadal change in ENSO asymmetry (i.e., nonlinearity) is also synchronized to the interdecadal

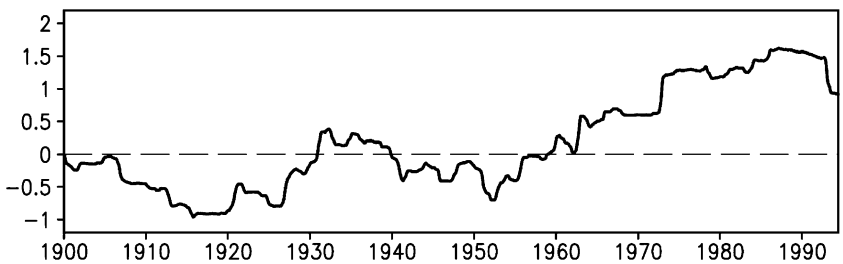

Fig. 7 Time series of the 21-year moving skewness of the Niño-3 index

Table 2 Summary for interdecadal changes in ENSO statistics

	Pre 1980s	Post 1980
Period	3–4 years	4–5 years
Amplitude	Small (s.t.d.=1.47)	Large (s.t.d.=1.67)
Propagation	Westward	Eastward/stationary
Structure	Toward the west	Toward the east
Skewness	Small	Large
Predictability	Less	More
NDH	Small	Large

(s.t.d. = standard deviation of Niño-3 index)

change in ENSO characteristics. Considering all these changes, it is natural to raise the question of how the changes in the characteristics of ENSO (i.e., the frequency, amplitude, asymmetry, and structure) and the changes in the background climate states are dynamically linked, and why are they synchronized?

A simple answer to the above questions may be found in Timmermann and Jin (2002a) and Timmermann et al. (2003). They explained the cause of decadal amplitude changes of ENSO based on nonlinear theory, using so-called 'homoclinic and heteroclinic connections'. Specifically, they showed that the nonlinearities in the tropical Pacific heat budget could lead to bursting behavior of the decadal occurrences of strong El Niño events, without invoking any external influence or stochastic forcing. However, although the regime for El Niño bursting is valid for a certain parameter range that is well matched to recent major El Niño events, it is limited and no bursting has occurred in a slight different parameter range. Thus, long-term changes in the ENSO characteristics should invoke changes in the background climate state, and the background climate state provides conditions for the atmosphere–ocean coupled instability and a parameter range that determines the behavior of ENSO bursting. Thus, in this section, the explanation on the interdecadal change in ENSO characteristics is given in the context of a linkage between the background change and its resultant change in ENSO behavior.

Kirtman and Schopf (1998) found that decadal variations in ENSO strength in a tropically confined system could be driven by small changes in the background mean states. Their point was further confirmed in the observational analysis by An and Jin (2000) and Wang and An (2001). By performing numerical experiments with a modified version of the "Cane-Zebiak" model (Zebiak and Cane 1987), in which the actual climate states are prescribed, Wang and An (2001, 2002) and An et al. (2006) analyzed how observed changes in the mean background state alter the characteristics of ENSO. They concluded that interdecadal changes in the background mean states explain the changes in amplitude, frequency, and canonical propagating features of ENSO. A similar conclusion was found by Fedorove and Philander (2001).

During the recent half century, there has been a significant decadal change in tropical climate states, in particular during a climate shift in the late 1970s (Nitta and Yamada 1989; Trenberth and Hurrel 1994; Wang and An 2001, 2002). Compared to the period before the climate shift, the mean surface wind stress after the climate shift is characterized by stronger equatorial westerlies in the western Pacific and easterlies in the eastern Pacific. There has been convergence in the central Pacific, and an increase in the mean tropical Pacific SST, particularly over the equatorial central Pacific and the southeastern tropical Pacific, where the rise in SST exceeds 0.5°C (Wang and An 2002). Fedorove and Philander (2001) emphasized the role played by the mean thermocline depth in inducing the change in ENSO behavior, but the reliability of the thermocline and subsurface temperature data was doubted by Wang and An (2001), since there is a shortage of long-term subsurface ocean data, particularly in the tropical central Pacific. After performing an eigenanalysis of a simple coupled ocean–atmosphere model, An and Jin (2000) proposed that the observed interdecadal change in the relative importance between the zonal advection effect, measured by the zonal gradient of mean SST ('zonal advection feedback'), and the vertical advection effect, measured by both mean upwelling and subsurface temperature change rate to the thermocline depth ('thermocline feedback'), could lead to the interdecadal change of ENSO modes. In other words, the observed climate shift could effectively modify the relative strengths of two major coupled feedbacks for the ENSO mode, the zonal advection and the thermocline feedbacks. These were decreased and increased, respectively, after the climate shift. This modification leads to a clearly distinctive change in the leading coupled mode (i.e., from an ENSO mode excited from the ocean-basin mode to one excited from a combined SST-ocean adjustment mode), in its frequency, growth rate, and spatial pattern, all of which are consistent with observation.

Theoretically, the zonal advection feedback is favorable to the generation of the westward-propagating ENSO mode, while the thermocline feedback promotes the eastward-propagating ENSO mode. This is because the maximum SST tendency driven by the zonal advection feedback is located in the western part of the existing SST maximum region, while that driven by the thermocline feedback is located in the eastern part. Furthermore, as mentioned in An and Jin (2004), the eastward-propagating ENSO events could facilitate the positive NDH, which would intensify the asymmetry of ENSO. Thus, as summarized in Fig. 8, the recent decadal changes in mean climate states provide a

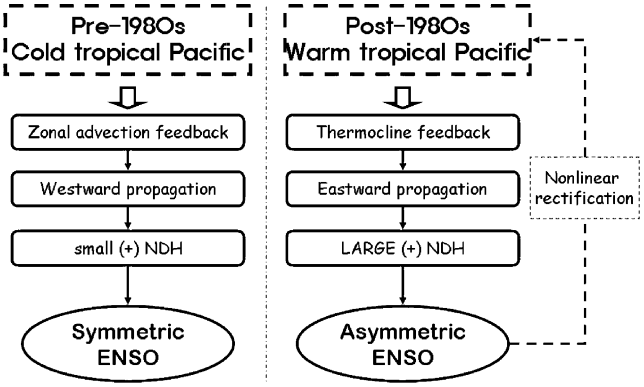

Fig. 8 Schematic diagram of the cause and effect for the interdecadal changes in the El Niño-La Niña asymmetry

favorable condition for thermocline feedback rather than for zonal advection feedback, resulting in a promotion of the eastward propagation of the ENSO mode. The eastward propagating ENSO mode easily produces a positive NDH, causing asymmetric ENSO events so that El Niño events are larger than La Niña events.

5 Concluding remarks

The ENSO nonlinearity expressed as the El Niño-La Niña asymmetry underwent a significant interdecadal variation. The interdecadal change in the ENSO nonlinearity can be attributed to either an internal nonlinear mechanism (Timmermann et al. 2003) or to changes in the background climate state. In this study, the latter case is emphasized, while still considering the former case. In particular, the ENSO bursting regime might be modified by the mean climate state; thus, to some extent, the interdecadal change in the mean climate states could result in favorable conditions for generating the ENSO bursting. As seen through observations, the decadal shift in mean climate state promotes the eastward propagation of the ENSO mode, thereby producing positive NDH which causes asymmetric ENSO events. Furthermore, the outputs from several coupled models also support the above argument, with results consistent with observations (An et al. 2005a).

Jin et al. (2003) quantitatively demonstrated that at least half of the increased tropical Pacific warming for recent

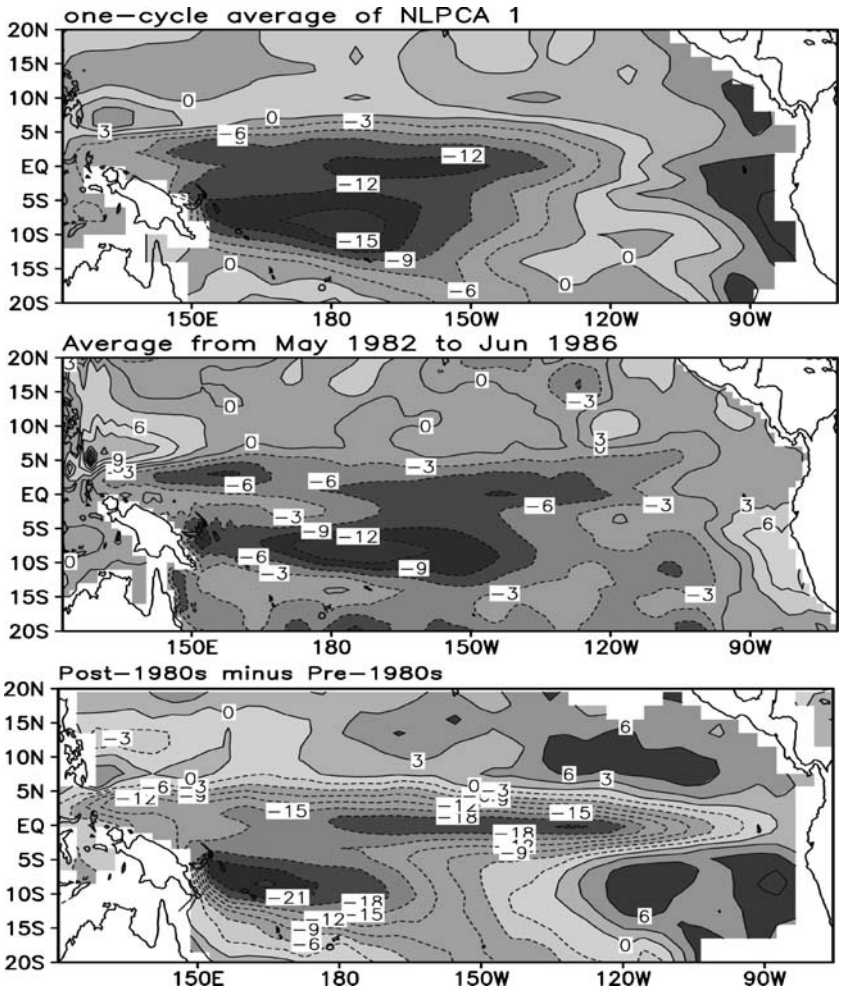

Fig. 9 Spatial patterns of thermocline anomalies obtained by integrating one complete cycle of the first NLPCA mode (upper panel); Averaging of thermocline anomalies between May 1982 and June 1986 (middle panel); and difference of thermocline between pre-1980s and post-1980s

decades was attributable to warming by NDH. With a qualitative approach, Rodgers et al. (2004) showed that the spatial patterns in SST representing El Niño-La Niña asymmetry strongly resemble those associated with decadal changes in SST, indicating that the decadal mean state of SST is due to a residual effect of the asymmetric ENSO variation. A similar result by An (2004) was obtained using a different data set and different approaches. This point was supported further by Monahan and Dai (2004), who analyzed several independent historical SST datasets. On the whole, these studies imply that the decadal variation in the tropical Pacific results partly from the nonlinear rectification of ENSO to the mean climate state (Fig. 8).

To provide evidence for the nonlinear rectification of ENSO, the nonlinear principal component analysis (NLPCA) was applied to thermocline anomalies in the tropical Pacific (An et al. 2005b). The NLPCA mode 1 of the thermocline anomalies reveals an asymmetric cycle (or nonlinear cycle) of ENSO (see Fig. 4 of An et al. 2005b). Using the first NLPCA mode, the residual effect of the nonlinear ENSO cycle is computed. As shown in Fig. 9, the residual after integrating one cycle of the first NLPCA mode (i.e., a canonical nonlinear ENSO cycle; uppermost panel of Fig. 9) is similar to the actual change in the thermocline between two decadal periods (pre-1980s vs. post-1980s). Furthermore, a simple average of thermocline anomalies from May 1982 to June 1986 over a complete ENSO cycle (middle panel) also exhibits similarity with the other two figures. Namely, the interdecadal change in the mean thermocline is attributable to the residual effect resulting from the asymmetric/nonlinear ENSO cycle. On the other hand, Schopf and Burgman (2006) raise an opposing argument to the aforementioned studies. Instead, they propose a mechanism in which the kinematic effect of oscillating a nonlinear temperature profile causes the Eulerian time mean temperature to mimic the observed changes in the mean SST, resulting in a skewness distribution of SST. However, changes in the propagating feature and evolution patterns of ENSO, and in the nonlinear/asymmetric ENSO cycle in terms of amplitude, are not fully understood under their mechanism.

Finally, the following studies proposed somewhat different views than those presented here; these are worth mentioning. Kleeman et al. (1999) and others (Gu and Philander 1997; Luo and Yamagata 2001; Holland et al. 2007) found that decadal variations originating from the subtropical Pacific, as opposed to those originating from the tropical Pacific, can affect the tropical Pacific through the oceanic meridional thermal advection or through other transport mechanisms, and thus can introduce decadal changes in ENSO properties. However, the primary cause of the Pacific decadal variation is still an open question. Thus, it is unclear which mechanism is the most influential in generating the tropical Pacific decadal variability, since both mechanisms likely have an effect on the tropical decadal variations. A quantitative comparison between all proposed mechanisms is beyond the scope of this paper, and should be a future objective for our research. Ye and Hsieh (2006) found that, in contrast to SST, the decadal change in the wind stress mean state did not bear resemblance to the wind stress anomalies found during El Niño, so the decadal change could not have been caused by the presence of stronger or more frequent El Niño episodes during the 1981–1995 period. In other words, there is a dynamic inconsistency between SST and wind stress anomalies in terms of their decadal change; this needs to be investigated in a future study. Also, beyond decadal changes, there are long-term trends from global warming that are not clearly defined (Vecchi et al. 2008). An et al. (2008) proposed the possibility of ENSO modulation during global warming due to a 'delayed' oceanic adjustment, in which changes in the ocean temperature profile lead to a modification of ENSO statistics. Further studies are required in this area.

Acknowledgments This research was supported by "National Comprehensive Measures against Climate Change" Program by Ministry of Environment, Korea (Grant No. 1700-1737-322-210-13), and by the Korea Research Foundation Grant funded by the Korean Government (MOEHRD, Basic Research Promotion Fund) (KRF-2007-313-C00784).

References

An S-I (2004) Interdecadal changes in the El Niño-La Niña symmetry. Geophys Res Lett 31:L23210. doi:10.1029/2004GL021699

An S-I (2008) Interannual variations of the tropical ocean instability wave and ENSO. J Climate 21:3680–3686

An S-I, Jin F-F (2000) An eigen analysis of the interdecadal changes in the structure and frequency of ENSO mode. Geophys Res Lett 27:2573–2576

An S-I, Jin F-F (2001) Collective role of thermocline and zonal advective feedbacks in the ENSO mode. J Climate 14:3421–3432

An S-I, Jin F-F (2004) Nonlinearity and asymmetry of ENSO. J Climate 17:2399–2412

An S-I, Kang I-S (2000) A further investigation of the recharge oscillator paradigm for ENSO using a simple coupled model with zonal mean and eddy separated. J Climate 13:1987–1993

An S-I, Wang B (2000) Interdecadal change of the structure of the ENSO mode and its impact on the ENSO frequency. J Climate 13:2044–2055

An S-I, Ham Y-G, Kug J-S, Jin F-F, Kang I-S (2005a) El Niño-La Niña asymmetry in the coupled model intercomparison project simulation. J Climate 18:2617–2627

An S-I, Hsieh WW, Jin F-F (2005b) A nonlinear analysis of the ENSO cycle and its interdecadal changes. J. Climate 18:3229–3239

An S-I, Ye Z, Hsieh WW (2006) Changes in the leading ENSO modes associated with the late 1970s climate shift: role of surface zonal current. Geophys Res Lett 33:L14609. doi:10.1029/2006GL026604

An S-I, Kug J-S, Ham Y-G, Kang I-S (2008) Successive modulation of ENSO to the future greenhouse warming. J Climate 21:3–21

Battisti DS, Hirst AC (1989) Interannual variability in a tropical atmosphere-ocean model: influence of the basic state, ocean geometry, and nonlinearity. J Atmos Sci 46:1687–1712

Bjerknes J (1966) A possible response of the atmospheric Hadley circulation to equatorial anomalies of ocean temperature. Tellus 18:820–829

Burgers G, Stephenson DB (1999) The 'Normality' of ENSO. Geophys Res Lett 26:1027–1030

Cane MA (1983) Oceanographic events during El Niño. Science 222:1189–1195

Cane MA, Zebiak SE (1985) A theory of El Niño and the Southern Oscillation. Science 228:1084–1087

Cane MA, Zebiak SE, Dolan SC (1986) Experimental forecasts of El Niño. Nature 321:827–832

Carton J, Chepurin G, Cao X, Giese B (2000) A simple ocean data assimilation analysis of the global upper ocean 1950–1995, Part 1: methodology. J Phys Oceanogr 30:294–309

Chang P, Wang B, Li T, Ji L (1994) Interactions between seasonal cycle and the Southern Oscillation: frequency entrainment and chaos in an intermediate coupled ocean-atmosphere model. Geophys Res Lett 21:2817–2820

Eisenman I, Yu L, Tziperman E (2005) Westerly wind bursts: ENSO's tail rather than the dog? J Climate 18:5224–5238

Fedorove AV, Philander SGH (2001) A stability analysis of tropical ocean-atmosphere interactions: bridging measurements and theory for El Niño. J Climate 14:3086–3101

Galanti E, Tziperman E, Harrison M, Rosati A, Giering R, Sirkes Z (2002) The equatorial thermocline outcropping -– A seasonal control on the tropical Pacific ocean-atmosphere instability strength. J Climate 15:2721–2739

Gu D, Philander SGH (1997) Interdecadal climate fluctuations that depend on exchanges between the tropics and extratropics. Science 275:805–807

Hansen DV, Paul CA (1984) Genesis and effects of long waves in the equatorial Pacific. J Geophys Res 89:10,431–10,440

Hoerling MP, Kumar A, Zhong M (1997) El Niño, La Niña, and the nonlinearity of their teleconnections. J Climate 10:1769–1786

Holland CL Scott RB, An S-I, Taylor FW (2007) Propagating decadal sea surface temperature signal identified in modern proxy records of the tropical Pacific. Climate Dyn 28:163–179

Jin F-F (1996) Tropical ocean-atmosphere interaction, the Pacific cold tongue, and the El Niño - Southern Oscillation. Science 274:76–78

Jin F-F (1997) An equatorial ocean recharge paradigm for ENSO. Part I: conceptual model. J Atmos Sci 54:811–829

Jin F-F, An S-I (1999) Thermocline and zonal advection feedbacks within the equatorial ocean recharge oscillator model for ENSO. Geophys Res Lett 26:2989–2992

Jin F-F, Neelin JD (1993) Modes of interannual tropical ocean-atmosphere interaction - a unified view. Part I: numerical results. J Atmos Sci 50:3477–3502

Jin F-F, Neelin JD, Ghil M (1994) El Niño on the devil's staircase: annual subharmonic steps to chaos. Science 264:70–72

Jin F-F, An S-I, Timmermann A, Zhao J (2003) Strong El Niño events and nonlinear dynamical heating. Geophys Res Lett 30:1120. doi:10.1029/2002GL016356

Jochum M, Murtugudde R (2004) Internal variability of the tropical Pacific ocean. Geophys Res Lett 31:L14309. doi:10.1029/2004GL020488

Kang I-S, Kug J-S (2002) El Niño and La Niña sea surface temperature anomalies: asymmetric characteristics associated with their wind stress anomalies. J Geophys Res 107 (D19):4372–4381

Kessler WS, Kleeman R (2000) Rectification of the Madden-Julian Oscillation into the ENSO cycle. J Climate 13:3560–3575

Kirtman BP, Schopf PS (1998) Decadal variability in ENSO predictability and prediction. J Climate 11:2804–2822

Kleeman R, McCreary JP, Klinger BA (1999) A mechanism for generating ENSO decadal variability. Geophys Res Lett 26:1743–1746

Legeckis R (1977) Long waves in the eastern equatorial Pacific ocean: a view from a geostationary satellite. Science 197:1179–1181

Luo J-J, Yamagata T (2001) Long-term El Niño-southern oscillation (ENSO)-like variation with special emphasis on the South Pacific. J Geophys Res 105:22,211–22,227

McPhaden MJ (1999) The child prodigy of 1997–1998. Nature 398:559–562

Monahan AH, Dai A (2004) The spatial and temporal structure of ENSO nonlinearity. J Climate 17:3026–3036

Neelin JD, Latif M, Jin FF (1994) Dynamics of coupled ocean-atmosphere models: the tropical problem. Annu Rev Fluid Mech 26:617–659

Neelin JD, Battisti D, Hirst AC, Jin FF, Wakata Y, Yamagata T, Zebiak SE (1998) ENSO theory. J Geophys Res C104:14262–14290

Nitta T, Yamada S (1989) Recent warming of tropical sea surface temperature and its relationship to the Northern Hemisphere circulation. J Meteor Soc Japan 67:375–383

Penland C, Sardeshmukh PD (1995) The optimal growth of tropical sea surface temperature anomalies. J Climate 8:1999–2024

Philander SGH (1983) El Niño Southern oscillation phenomena. Nature 302:295–301

Philander SGH (1990) El Niño, La Niña, and the Southern Oscillation. Academic Press, San Diego, CA, 293 pp

Qiao L, Weisberg RH (1998) Tropical instability wave energetics: observations from the tropical instability wave experiment. J Phys Oceanogr 28:345–360

Rasmusson EM, Wallace JM (1983) Meteorological aspects of the El Ninõ/Southern Oscillation. Science 222:1195–1202

Reynolds RW, Smith TM (1994) Improved global sea surface temperature analysis using optimum interpolation. J Climate 7:929–948

Rodgers KB, Friederichs P, Latif M (2004) Tropical Pacific decadal variability and its relation to decadal modulations of ENSO. J Climate 17:3761–3774

Schopf PS, Burgman RJ (2006) A simple mechanism for ENSO residuals and asymmetry. J Climate 19:3167–3179

Schopf PS, Suarez MJ (1988) Vacillations in a coupled ocean-atmosphere model. J Atmos Sci 45:549–566

Smith TM, Reynolds RW (2004) Improved extended reconstruction of SST (1854–1997). J Climate 17:2466–2477

Suarez MJ, Schopf PS (1988) A delayed action oscillator for ENSO. J Atmos Sci 53:2786–2802

Swenson MS, Hansen DV (1999) Tropical Pacific ocean mixed layer heat budget: the Pacific cold tongue. J Phys Oceanogr 29:69–82

Thompson CJ, Battisti DS (2000) A linear stochastic dynamical model of ENSO. Part I: model development. J Climate 14:445–466

Timmermann A, Jin FF (2002a) A nonlinear mechanism for decadal El Niño amplitude changes. Geophys Res Lett 29:1003. doi:10.10129/2001GL013369

Timmermann A, Jin FF (2002b) Phytoplankton influences on tropical climate. Geophys Res Lett 39. doi:10.10129/2002GL15434

Timmermann A, Jin FF, Abshagen J (2003) A nonlinear theory for El Niño bursting. J Atmos Sci 60:152–165

Trenberth KE, Hurrel JW (1994) Decadal atmosphere-ocean variations in the Pacific. Climate Dyn 9:303–319

Tziperman E, Stone L, Cane M, Jarosh H (1994) El Niño chaos: overlapping of resonances between the seasonal cycle and the Pacific ocean-atmosphere oscillator. Science 264:72–74

Vecchi GA, Clement A, Soden BJ (2008) Examining the tropical Pacific's response to global warming. Eos Trans AGU 89(9):81–83

Vialard J et al (2001) A model study of oceanic mechanisms affecting equatorial Pacific sea surface temperature during the 1997–98 El Niño. J Phys Oceanogr 31:1649–1675

Waliser DE, Graham NE (1993) Convective cloud systems and warm-pool SSTs: coupled interactions and self-regulation. J Geophys Res 98:12881–12893

Wang B (1995) Interdecadal changes in El Niño onset in the last four decades. J Climate 8:267–285

Wang B, An SI (2001) Why the properties of El Niño changed during the late 1970s. Geophys Res Lett 28:3709–3712

Wang B, An SI (2002) A mechanism for decadal changes of ENSO behavior: roles of background wind changes. Climate Dyn 18:475–486

Wang W, McPhaden MJ (2000) The surface-layer heat balance in the equatorial Pacific Ocean. Part II: interannual variability. J Phys Oceanogr 30:2989–3008

Weisberg RH, Weingartner TJ (1988) Instability waves in the equatorial Atlantic Ocean. J Phys Oceanogr 18:1641–1657

White HG (1980) Skewness, kurtosis and extreme values of Northern Hemisphere geopotential heights. Mon Wea Rev 108:1446–1455

Wilson D, Leetmaa A (1988) Acoustic Doppler current profiling in the equatorial Pacific in 1984. J Geophys Res 93:13947–13966

Wu A, Hsieh WW (2003) Nonlinear interdecadal changes of the El Niño-Southern Oscillation. Climate Dyn 21:719–730

Wyrtki K (1985) Water displacements in the Pacific and the genesis of El Niño cycles. J Geophys Res C90:7129–7132

Ye Z, Hsieh WW (2006) The influence of climate regime shift on ENSO. Clim Dynam 26:823–833

Yu JY, Liu WT (2003) A linear relationship between ENSO intensity and tropical instability wave activity in the eastern Pacific Ocean. Geophys Res Lett 30:14,1735. doi:10.1029/2003GL017176

Zebiak SE, Cane M (1987) A model El Niño/Southern Oscillation. Mon Weather Rev 115:2262–2278